Journal Homepage: http://ijcpe.uobaghdad.edu.iq
Iraqi Journal of Chemical and Petroleum Engineering
Vol. 27 No. 2 (June 2026) 77 – 88
EISSN: 2618-0707, PISSN: 1997-4884

Fixed bed adsorption of nitrate and phosphate nutrients using char prepared by co-pyrolysis of waste tires and date stones

Sally Ali Hussein [a, *], Muthanna J. Ahmed [a]

a Chemical Engineering Department, College of Engineering, University of Baghdad, Baghdad, Iraq

Abstract

Conversion of waste tires and date stones into char through co-pyrolysis is an effective way to safely remove and recycle these materials. This study tested char as a low-cost adsorbent for removing nitrate and phosphate in fixed-bed systems, offering a way to reuse waste tires and date stones. The effects of inlet pollutant concentration (50, 150, and 300 mg/L), flow rate (5, 10, and 15 ml/min), and bed height (5, 10, and 15 cm) on the adsorption system's breakthrough were measured. Characteristics of char were analyzed via the Fourier transform of infrared (FTIR), Brunauer-Emmett-Teller (BET), and zeta potential. The fixed-bed analysis demonstrated superior correlation of breakthrough data with both the Yoon-Nelson and Thomas models. Under varying circumstances, the findings agreed with the Yoon-Nelson and Thomas models, as measured by the correlation coefficient R^2 values (0.8147-0.9913) for phosphate, (0.9187-0.9913) for nitrate, and (0.8146-0.9907) for phosphate, (0.9189-0.9801) for nitrate, respectively. The results demonstrate the potential of the prepared char as an efficient and sustainable adsorbent for nutrient removal in continuous treatment systems, providing a promising approach for wastewater treatment and waste valorization.

Keywords: Fixed bed adsorption; Breakthrough curves; Binary pollutants; Anion adsorption; Co-pyrolysis.

Received on 25/11/2025, Received in Revised Form on 25/05/2026, Accepted on 26/06/2026, Published on 30/06/2026

https://doi.org/10.31699/IJCPE.2026.2.7

1- Introduction

The lack of access to drinkable water is a global epidemic and a big problem for many people. Potable water has become increasingly important in the modern era due to its crucial role in human consumption and other uses [1, 2]. Unless it has been treated, surface water should not be consumed. To meet drinking water requirements, it is essential to purify surface water [3].

Nitrate and phosphate contamination of water sources is a serious worldwide issue. Humans need certain non-renewable micronutrients to function. At low concentrations, these substances are harmless, but at high levels, they become deadly [4]. When released into natural water sources, the nutrient-rich anionic contaminants phosphate, nitrite, and nitrate dramatically decline water quality [5].

As fertilizers, nitrate and phosphate are essential to contemporary agriculture because they provide plants with the nutrients they require to flourish. These elements are also critical to the development of all living things. In excess, they can reduce the amount of dissolved oxygen (DO), decrease water quality, generate algal blooms on the water's surface, and lead to other types of plankton, eventually leading to eutrophication issues [6].

In many developing countries, nitrates are the main problem with groundwater contamination. Many human activities have contributed to the rise in nitrate concentrations, the most common being the widespread use of urea and other nitrogen fertilizers in agricultural environments. Although fertilizer usage has increased, agricultural productivity has also increased, which is crucial for feeding a growing population [7]. Nitrogen fertilizer, however, has a very low usable range (only 30–50%) owing to its high-water solubility. Although nitrate is more soluble in water than other forms of nitrogen, it does not bind to soil immediately; instead, it leaches into the ground rather than being adsorbed [5]. As a result, ground and surface water sources become more polluted with nitrates. Nitrate contamination comes from point and nonpoint sources, including inadequately treated industrial effluents, agricultural and urban runoff, landfill leachate, malfunctioning septic tanks, and unprocessed domestic sewage and animal waste [6].

Phosphate is essential for the eutrophication of our valuable natural water. Orthophosphate is the predominant form of phosphate in wastewater from municipalities and factory wastewater [8, 9]. Due to the health and environmental risks that high concentrations of nitrates and phosphates in water may cause, the World Health Organization has set permissible limits for these two substances to ensure water safety and protect human health; the maximum permissible limit for nitrates has been set at 50 mg/L, and for phosphates at 0.5 mg/L [10]. The demand for methods to remove phosphate and nitrate has increased due to stricter environmental regulations.

*Corresponding Author: Email: sally.ali2107m@coeng.uobaghdad.edu.iq

Some of the methods include electrocoagulation [11], Ion Exchange [12], and adsorption [13].

Among all techniques, adsorption is the most effective method for removing nutrients and similar compounds from wastewater. Adsorption techniques mitigate detrimental consequences and allow the adsorbent to be recycled [14, 15].

The identification of novel adsorbents capable of efficiently removing phosphate and nitrate from water-based solutions is a challenge for adsorption technology. Examples of such adsorbents include zeolite [16], clays [17], chitosan [18], and char [13, 19].

Recently, several studies have investigated the removal of nitrate and phosphate using various adsorbents, including modified biochar, zeolite, and chitosan-based materials. However, most of these studies were conducted using batch adsorption systems. Limited research has focused on the simultaneous removal of nitrate and phosphate in continuous fixed-bed column systems, which are more relevant for practical water treatment applications. Furthermore, the use of co-pyrolyzed waste materials, particularly waste tires combined with agricultural biomass, remains relatively unexplored for nutrient removal. Therefore, developing low-cost adsorbents from waste materials for efficient binary nutrient removal in fixed-bed systems is still an important research challenge.

Char is a solid substance with a high carbon content. Biochar production relies on three key factors: the manufacturing process (including methods and temperature), the type of biomass (such as rice hulls, food waste, animal by-products, various solid wastes), and the manufacturing technology (including pyrolysis, thermal carbonization, and gasification) [20].

Pyrolysis is a thermochemical conversion process that converts biomass or organic material into liquid (bio-oil), solid (biochar), and gaseous products (syngas) by heating in an anaerobic atmosphere; therefore, Pyrolysis is a more environmentally sustainable option compared to combustion [21]. The use of co-pyrolysis has increased in recent years as a possible remedy for the issue of inferior pyrolysis byproducts. Therefore, Co-pyrolysis resembles pyrolysis and includes the simultaneous pyrolysis of more than one biomass or waste material [22].

In this study, a mixture of 25% WT and 75% DS was co-pyrolyzed at 700 °C for 120 minutes to produce char. The resulting char was then used in a fixed-bed adsorption system to remove nitrate and phosphate from a binary solution. The selection of the 25% WT and 75% DS mixture was based on preliminary experimental investigations conducted by the authors to optimize the physicochemical properties and adsorption performance of the produced char.

2- Materials and methods

2.1. Preparation and characterization of adsorbents

Date stones (DS) and waste tires (WT) used in this study were collected from Baghdad, Iraq, for char preparation. The materials were oven-dried at 100 °C and 105 °C for 12 hr, then sieved to obtain particles between 2 and 1.7 mm. A mixture of 25% WT and 75% DS was co-pyrolyzed in a sealed muffle furnace at 700 °C for 120 min, as shown in Fig. 1.

After cooling to room temperature, the char samples were washed with distilled water, and the char product was dried at 100 °C for 24 hr. The yield of char was determined in Eq. 1 as follows:

$$yield\ \% = \frac{W_f}{W_o} * 100 \quad (1)$$

Where W_f and Wo are the weights of the char product and blend of WT and DS, respectively.

The pore size and surface area of the adsorbent were evaluated using the Brunauer-Emmett-Teller (BET) method on a Micromeritics ASAP 2400 instrument for nitrogen adsorption-desorption at 77 K. The Fourier transform infrared (FTIR) spectra was obtained in absorbance mode over 4000-400 cm^{-1} using the KBr pellet method. The zeta potential of the surface charge of char was measured using a zeta potential analyzer (Brookhaven, 2013, USA).

2.2. Fixed Bed Column Experiments

The Pyrex glass tube that makes up the fixed-bed column is 39.5 cm high, 17.6 mm in outside diameter, and 14 mm in inner diameter, as shown in Fig. 2. At the foot of the column, a single layer of material was fastened around a stainless-steel sieve. The required adsorbent bed height was achieved by packing a specific amount of the produced char into the column. This quantity may be 5, 10, or 15 cm, equal to 3,0507, 6,0971, or 8.7511 g of char, respectively.

Afterwards, the column was reinforced to ensure a consistent flow of the solution. A dosing pump was employed to regulate the flow rate of a binary NO_3^{-1}/PO_4^{-3} solution at 5, 10, and 15 mL/min while being pumped upstream through the column (WATSON-MARLOW LIMITED/FLAMOUTH CORNWELL ENGLAND). The solution concentrations were 50, 150, and 300 ppm. Ion chromatography (IC) (Cecil, 2014) was employed to quantify the concentration of a binary NO_3^{-1}/PO_4^{-3} solution obtained at different intervals from the column effluent.

For the analysis of experimental breakthrough curves, two common models, the Yoon-Nelson models [23] Thomas model [24], were applied in Eq. 2 and Eq. 3:

$$\ln \frac{C_t}{C_o - C_t} = K_{YN} * t - \tau * K_{YN} \quad (2)$$

$$\ln\left(\frac{C_o}{C_t} - 1\right) = \frac{K_{TH} q_o w}{Q} - K_{TH} C_o t \quad (3)$$

Where K_{YN} (min^{-1}) is the Yoon-Nelson constant rate, τ (min) is the time required for 50% adsorbate breakthrough. K_{Th} (mL/min.mg) is the Thomas rate constant; Q (mL/min) the flow rate, q_o (mg/g) is the equilibrium nutrient uptake per g of the adsorbent (char);

W (g) the mass of adsorbent, C_o (mg/L) is the inlet nutrient concentration; C_t (mg/L) is the outlet concentration at time t, and t total (min) stands for flow time.

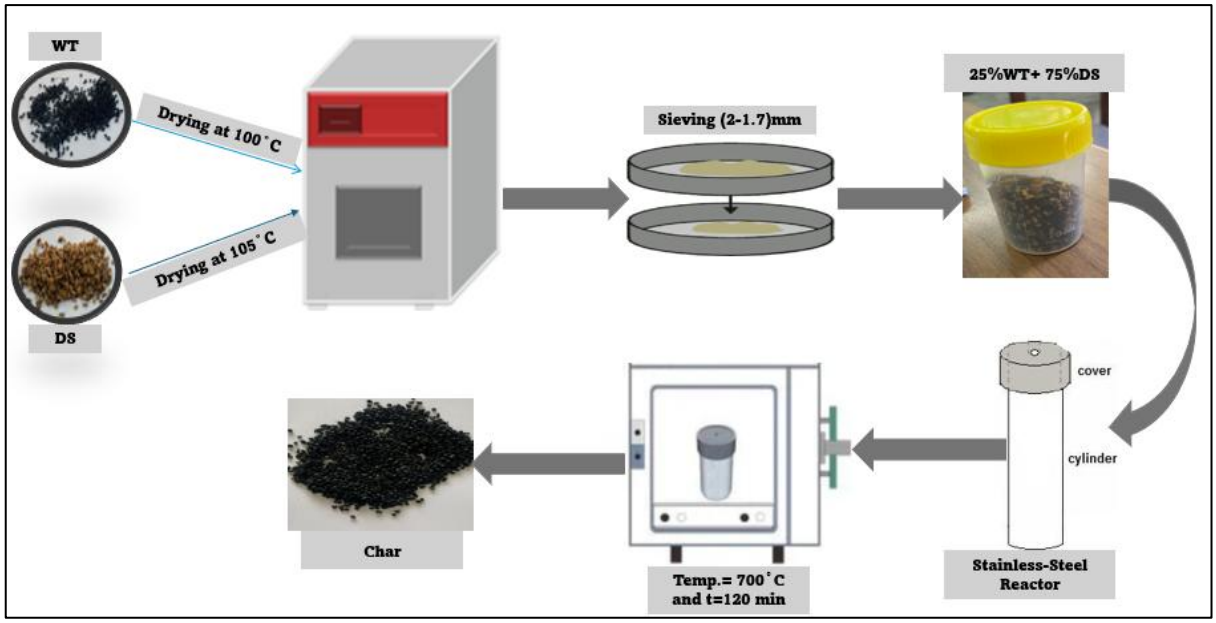

Fig. 1. Steps of char production from waste

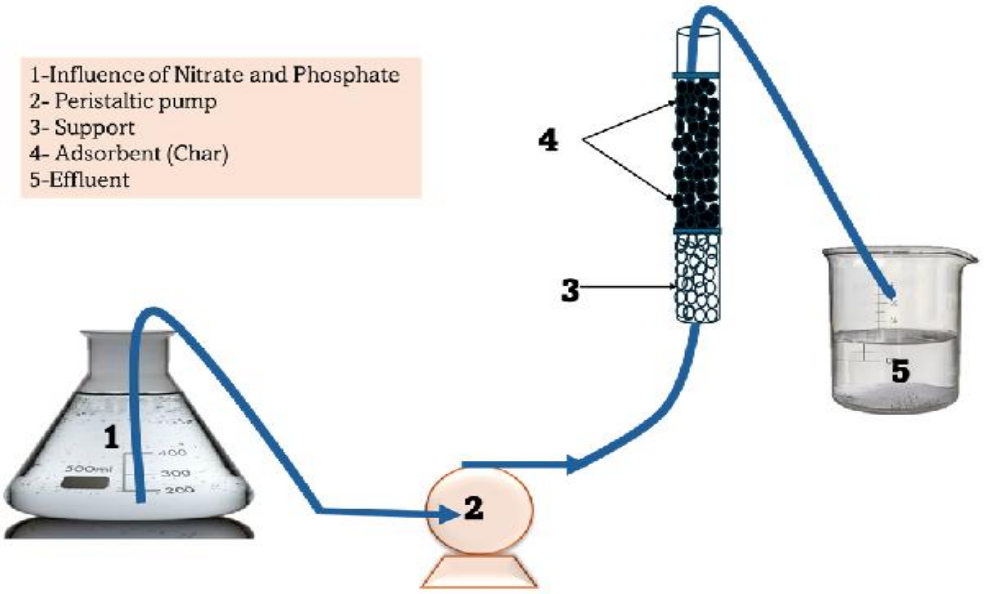

Fig. 2. Fixed bed column schematic diagram for adsorption of PO_4^{-3} and NO_3^{-1}

3- Results and discussion

3.1. Characterization of char

The char produced from co-pyrolyzing 25% WT and 75% DS has a yield of 24.45%, as shown in Eq.1. Important adsorbent properties are surface area, total pore volume, and average pore diameter. In this study, Fig. 3 illustrates the specific surface area and the N_2 adsorption isotherm of the 25% WT + 75% DS composite. The char has a surface area of 200.96 m^2/g, a pore volume of 0.1426 cm^3/g, and an average pore diameter of 2.84 nm. According to IUPAC standards, this average pore diameter means the char is mesoporous. Mesoporous char is useful for applications with large molecules. The relatively high surface area and mesoporous structure provide a large number of active sites and facilitate the diffusion of nitrate and phosphate ions into the internal pores of the adsorbent.

The surface charge of char affects adsorption capacity by influencing electrostatic interactions. The surface of prepared char is strongly dependent on the solution pH owing to the protonation and deprotonation of surface functional groups such as hydroxyl and carboxyl groups. Under the highly acidic conditions at pH = 2, these functional groups become protonated, resulting in a

positively charged surface. This positively charged surface significantly enhances the electrostatic attraction between the adsorbent and negatively charged nitrate and phosphate ions. In addition, phosphate ions have a higher negative charge compared to nitrate ions and may exhibit stronger interaction with the adsorbent surface, leading to competitive adsorption behavior in the binary system. To measure the zeta potential, 0.2 g of char was added to 50 mL of purified water at pH 7.5±0.5. The zeta potential changes with solution pH; char has a negative zeta potential (from -10 to -40 mV) in neutral to slightly acidic conditions, and a positive zeta potential in basic solutions. Fig. 4 shows that the char's surface has a negative zeta potential of -34.84 mV [25,26].

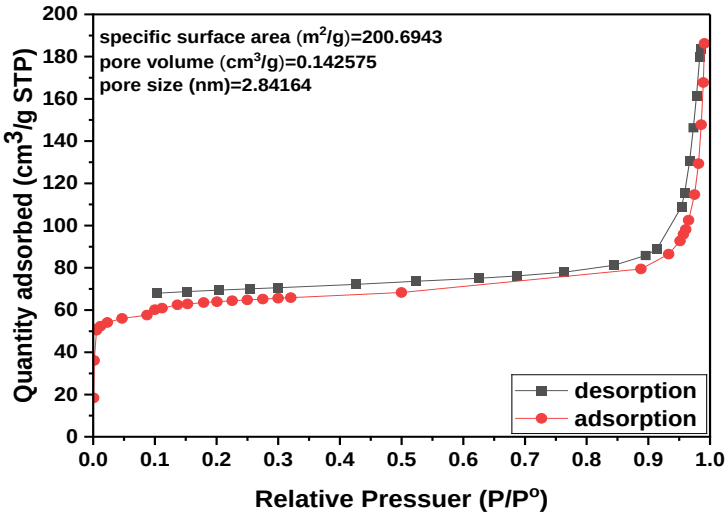

Fig. 3. N_2 adsorption-desorption isotherm of composite (25%WT+75%DS)

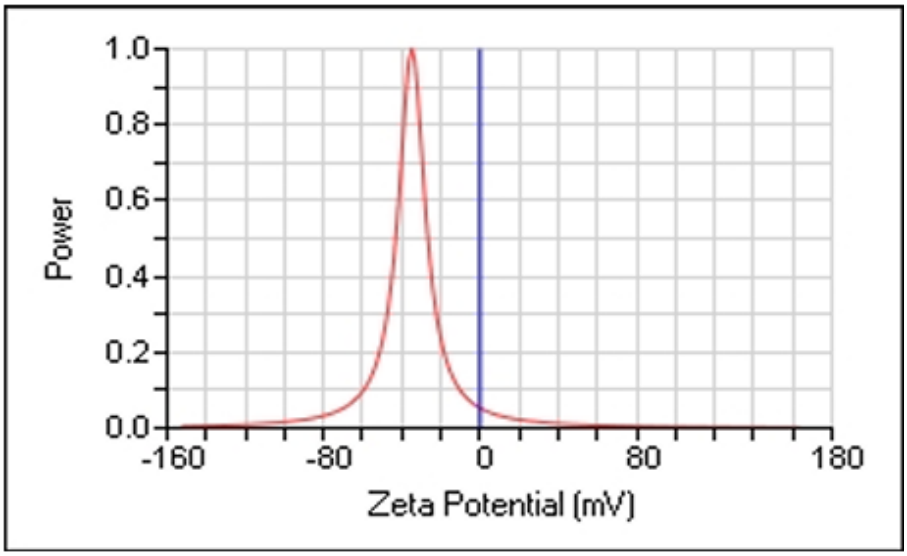

Fig. 4. Zeta potential of char

One important factor in char's adsorption capacity is the surface groups it contains. The surface characteristics of char, both before and after it absorbs pollutants such as PO_4^{-3} / NO_3^{-1}, can be studied using Fourier transform infrared spectroscopy, as shown in Fig. 5. A char surface is indicated by the presence of many functional groups, as seen by peaks in the 400-4000 cm^{-1} range, and the OH stretching vibration at 3419 cm^{-1} [27]. The peak indicated a carbonyl (C=O) group stretching at 1722 cm^{-1}, while the peak indicated the aliphatic C-H bond at 2964.36 cm^{-1} [28]. After the PO_4^{-3} / NO_3^{-1}(binary) mixture was adsorbed, the FTIR analysis showed a decrease in peak intensity. This was caused by interactions with phosphate and nitrate, as well as hydrogen bonds assisted by functional groups on the char surface. There were also alterations in the spectrum, with peaks losing their association with carboxyl and hydroxyl groups and peaks moving around. The peak at 2358 cm^{-1} disappeared because of the interaction between PO_4^{-3} and NO_3^{-1}. The peak at 1615 cm^{-1} (C-C) emerges following the adsorption of a binary (PO_4^{-3} / NO_3^{-1}), indicating the creation of a group with a function on the char surface [25]. The presence of hydroxyl and carbonyl functional groups facilitates adsorption through hydrogen bonding and electrostatic interactions with nitrate and phosphate ions.

3.2. Continuous adsorption

The breakthrough point was defined as Ct/Co = 0.05, while column exhaustion was considered at Ct/Co = 0.95. The region between these two points represents the mass transfer zone (MTZ), which describes the active adsorption zone inside the column. Table 1 shows the summarized main operating conditions used in the fixed-bed column.

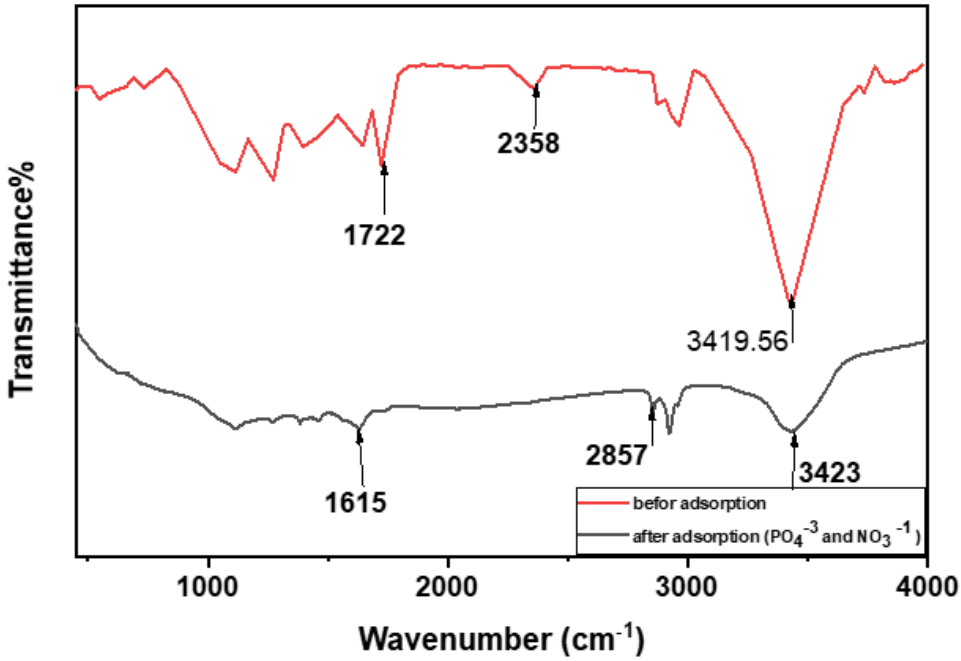

Fig. 5. FTIR before and after adsorption of the binary component

Table 1. Nutrient Adsorption in a Fixed Bed Column Operating at 25 °C

Parameters	Bed height (cm)	Initial binary concentration of nitrate and phosphate (mg/L)	Flow rate (mL/min)
Initial Concentration	10	100	10
	10	300	10
	10	600	10
Flow Rate	10	300	5
	10	300	10
	10	300	15
Bed Height	5	300	10
	10	300	10
	15	300	10

3.2.1. Effect of initial nutrient concentration

The different initial concentrations (50, 150, and 300 mg/L) on breakthrough curves are shown in Fig. 6, under an adsorption condition of 10 cm bed height and a flow rate of 10 mL/min. The bed becomes saturated more quickly at higher nutrient concentrations, leading to earlier breakthrough time. A longer contact time is required to attain adsorption equilibrium at lower initial solute concentrations, as evidenced by the inverse relationship between the two variables. Since diffusion limits the adsorption rate, variables that influence diffusion have a major bearing on it. The elevated inflow concentration led to effectively occupied adsorption sites, resulting in a more pronounced breakthrough curve and accelerating bed saturation [27-29].

3.2.2. Effect of flow rate

The adsorption breakthrough curves for NO_3^{-1} and PO_4^{-3} onto char are examined at volumetric flow rates of 5, 10, and 15 mL/min, with an inlet nutrient concentration of 150 mg/L and a bed length of 10 cm, as shown in Fig. 7. At a volumetric flow rate of 15 mL/min, the statistical analysis shows that anions are rapidly removed initially, but the rate gradually decreases until saturation is reached. This can indicate a higher flow rate, which would shorten breakthrough and fatigue times and enhance the mass transfer zone. Poor liquid distribution throughout the fixed bed and insufficient time for lateral diffusion inside the char bed are consequences of an increase in the volumetric flow rate, which shortens the contact duration between the adsorbate and adsorbent. The result is a decrease in the boundary layer and an

increase in the mass transfer resistance associated with adsorption within the bed, as there is less solute diffusion between the adsorbent particles and the surrounding liquid film [30].

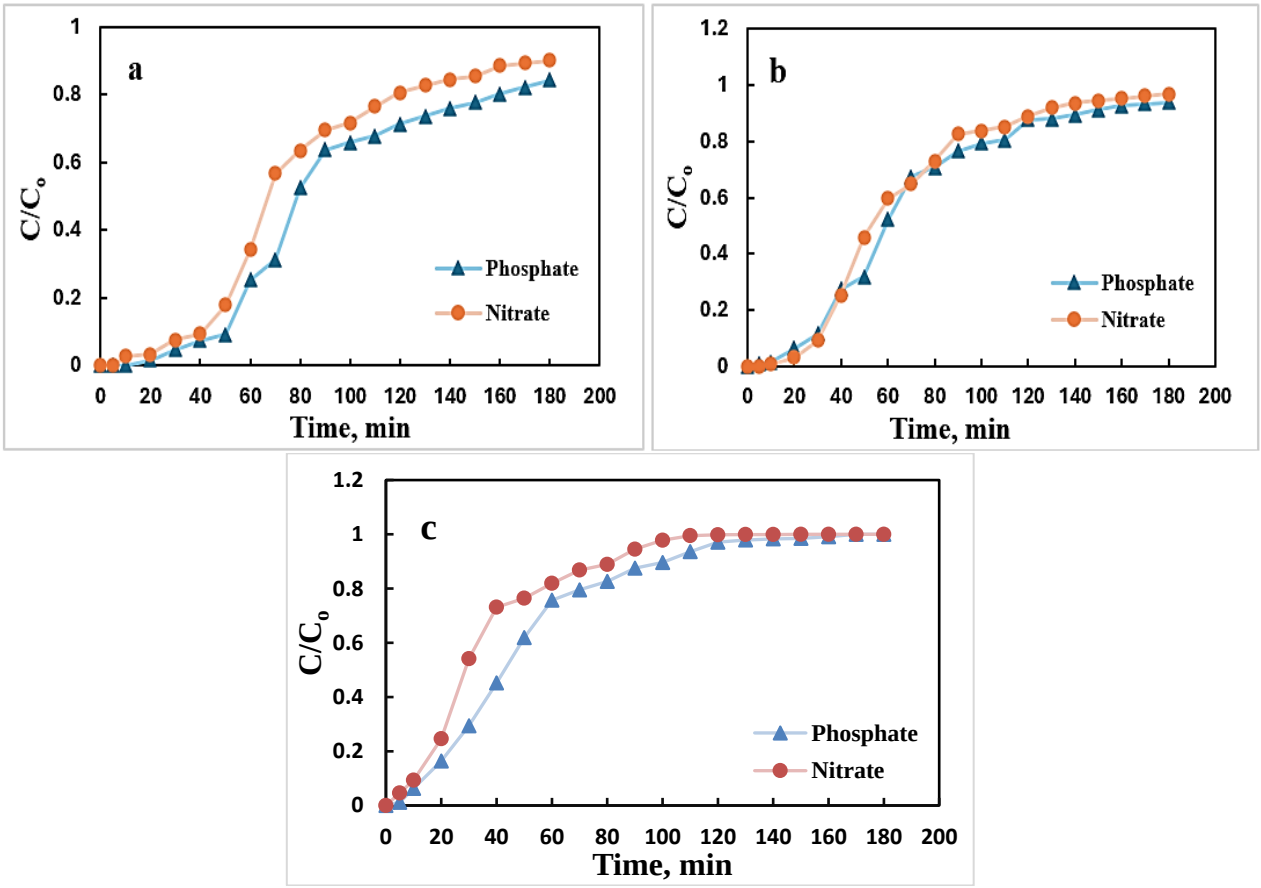

Fig. 6. Experimental breakthrough curves at different inlet concentrations of binary component solution of char at (a=50 mg/L, b=150 mg/L, and c=300 mg/L, H=10 cm, and Q=10 mL/min, pH=2)

3.2.3. Effect of bed height

The bed height is the main parameter in the configuration of fixed-bed adsorption columns. The elevation of the bed is essential when building a bed with a stationary adsorption column. The curves for the breakthrough of different bed heights of char (5, 10, and 15 cm) at a flow rate of 10 mL/min and an initial concentration of 150 mg/L are shown in Fig. 8. It is evident that the time to breakthrough and resistance time of the substance in the column increase as the bed length increases, allowing molecular molecules to penetrate the adsorbent particles. Conversely, the bed becomes saturated more rapidly at reduced heights than at elevated ones. Alongside an augmentation in bed length, a rise in the total quantity of binding sites enhances the adsorption area of the adsorbent [30-32].

3.3. Breakthrough curve modelling

Predicting the effluent breakthrough curve is crucial for the successful design and operation of fixed-bed column systems. Hence, the Yoon-Nelson and Thomas models are used to analyze experimental breakthrough data for nitrate and phosphate adsorption on char to ascertain the dynamic behavior in the fixed-bed column shown in Table 2 and Table 3. The linear regression tools in Microsoft Excel (Data → Solver) are used to generate analytical results with constants from two models, Eqs. 2 and 3.

At the analyzed fixed-bed conditions, the results demonstrate that Yoon-Nelson and the Thomas models provide better correlations for breakthrough data, with high R^2 values for Yoon- Nelson (0.9187-0.9913) and (0.8147-0.9913) for NO_3^{-1} and PO_4^{-3}, respectively; and for the Thomas model, R^2 values (0.9189-0.9901) and (0.9058-0.9907) for NO_3^{-1} and PO_4^{-3}, respectively. Additionally, the rate of adsorption decrease is directly related to the breakthrough for NO_3^{-1} or PO_4^{-3}adsorption on char.

Fig. 9 shows the predicted breakthrough results for NO_3^{-1} and PO_4^{-3} adsorption using these models under specific conditions: an inlet concentration of 150 mg/L, a flow rate of 10 mL/min, and a bed height of 10 cm. The experimental values of q_o (mg/g) for the Thomas model confirm that the adsorption capabilities of both nutrients decrease with increasing bed height, and that it increases with increasing inlet concentration and flow rate. The values of the parameter τ for the Yoon-Nelson model also show that breakthrough time decreases with increasing

flow rate and inlet concentration, and it increases with increasing bed height [33, 34].

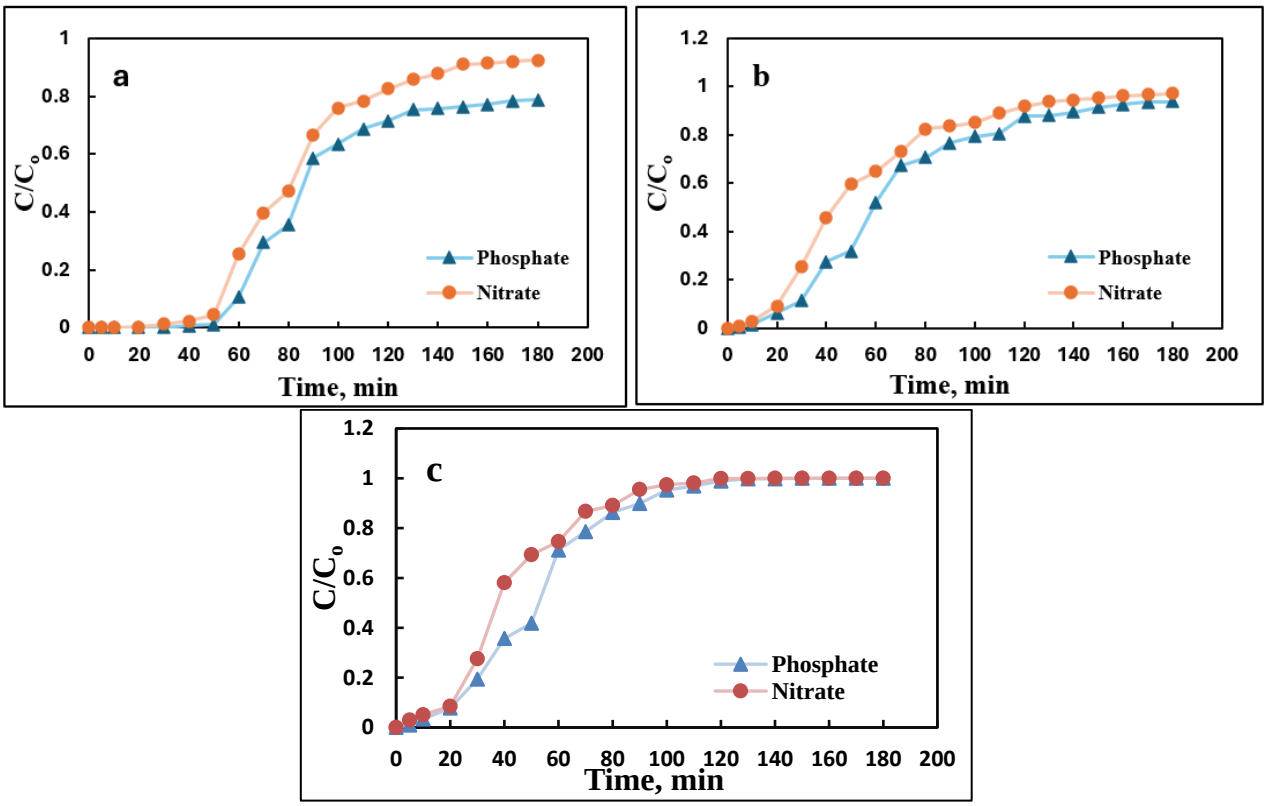

Fig. 7. Experimental breakthrough curves at different flow rates of binary component solution of char at (a=5 mL/min, b=10 mL/min, and c=15 mL/min, H=10 cm, Conc.=150 mg/L, pH=2)

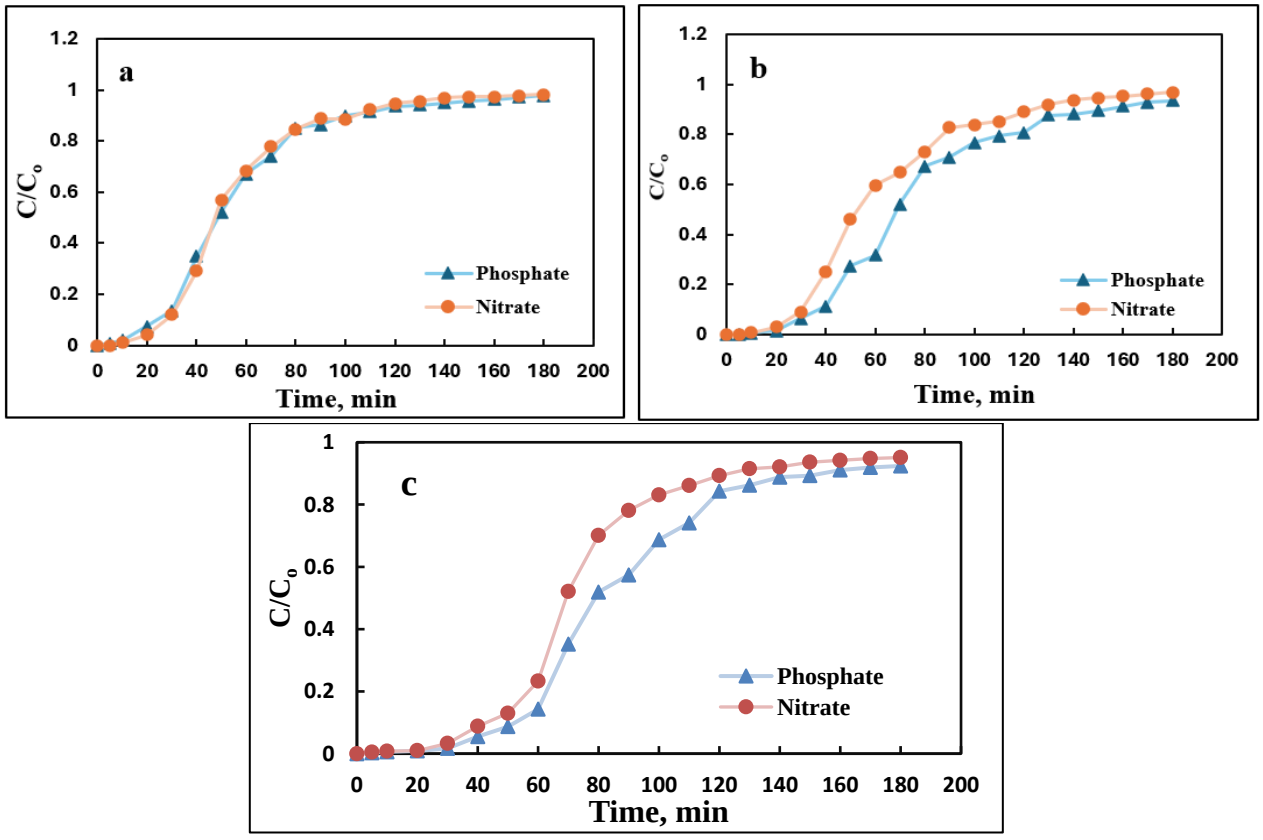

Fig. 8. Experimental breakthrough curves at different bed heights of binary component solution of char at (a=5 cm, b=10 cm, and c=15 cm, Q=10mL/min, conc.=150 mg/L, pH=2)

Table 2. Yoon-Nelson parameters under various circumstances by use of linear regression analysis

Inlet concentration (mg/L)	Char bed height (cm)	Flow rate (ml/min)	K_{YN} (1/min)		τ (min)		R^2	
			PO_4^{-3}	NO_3^{-1}	PO_4^{-3}	NO_3^{-1}	PO_4^{-3}	NO_3^{-1}
50	10	10	0.0333	0.0346	105.18	90.82	0.9061	0.9242
150	10	10	0.0392	0.0396	81.80	65.85	0.9191	0.9196
300	10	10	0.0500	0.0701	54.59	38.62	0.9635	0.9624
150	5	10	0.0430	0.0420	68.22	54.51	0.9237	0.9202
150	15	10	0.0489	0.0493	101.13	89.83	0.9407	0.9913
150	10	5	0.0475	0.0493	118.36	100.52	0.8147	0.9187
150	10	15	0.0781	0.0736	46.23	55.11	0.9913	0.9411

Table 3. The parameters of Thomas' model are applied in various contexts through linear regression analysis

Inlet concentration (mg/L)	Char bed height (cm)	Flow rate (ml/min)	K_{Th} (mL/min.mg)		q_o (mg/g)		R^2	
			PO_4^{-3}	NO_3^{-1}	PO_4^{-3}	NO_3^{-1}	PO_4^{-3}	NO_3^{-1}
50	10	10	0.6660	0.6920	8.63	7.45	0.9058	0.9241
150	10	10	0.2610	0.2630	20.13	16.20	0.9190	0.9195
300	10	10	0.1667	0.2337	26.86	19.00	0.9635	0.9624
150	5	10	0.2867	0.2800	33.54	26.80	0.9237	0.9202
150	15	10	0.3233	0.3287	17.29	15.40	0.9422	0.9228
150	10	5	0.3167	0.3287	14.56	12.36	0.8146	0.9189
150	10	15	0.4900	0.5200	20.34	17.06	0.9907	0.9801

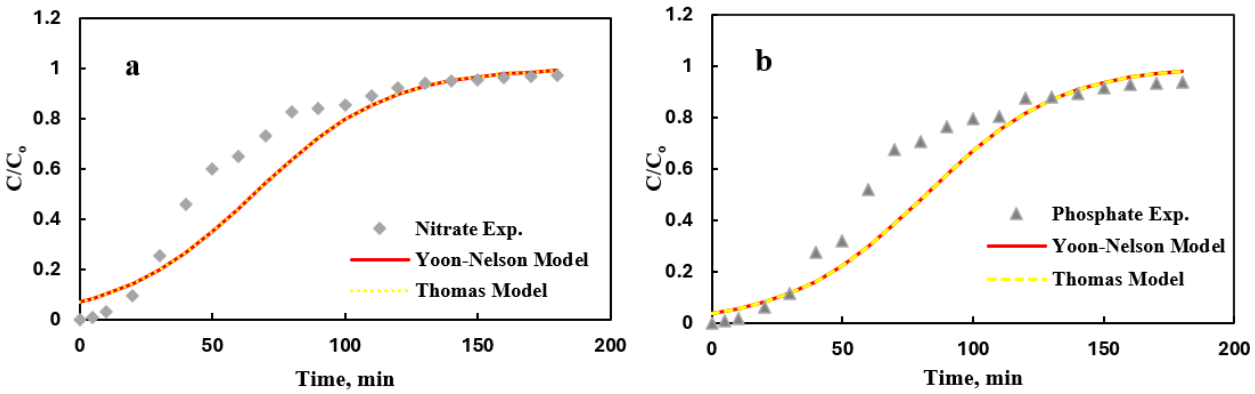

Fig. 9. Experimental and predicted breakthrough curves for NO_3^{-1} and PO_4^{-3}

Table 4 compares the adsorption performance of the prepared WT–DS char with several previously reported adsorbents, such as zeolite and modified biochars. The results indicate that the prepared char exhibits competitive adsorption capacity for both nitrate and phosphate removal. It should be noted that many previous studies were conducted in batch systems, whereas the present study evaluates the adsorption performance in a continuous fixed-bed column, which is more relevant for practical wastewater treatment applications.

Table 4. Comparison with previous adsorbents

Adsorbent	pollutant	System	Adsorption capacity mg/g	Reference
Surfactant-modified Zeolite	NO_3^{-1}	Fixed bed column	0.07-0.74	[35]
Acid-modified biochar (Prosopis juliflora)	NO_3^{-1}	Fixed bed column	8.51	[36]
25%WT+75%DS	NO_3^{-1}	Fixed bed	26.8	This study
25%WT+75%DS	PO_4^{-3}	Fixed bed column	33.54	This study

4- Conclusions

The co-pyrolysis of waste tire/date stone blends into char and its application as an adsorbent to remove binary phosphate and nitrate from aqueous solutions using a fixed-bed adsorption column were investigated. The prepared char had a high surface area (200.6943 m^2/g) and several functional groups. Reducing the binary PO_4^{-3} / NO_3^{-1} inlet concentration, increasing the char bed height, and decreasing the feed flow rate all improved the fixed-bed adsorption system's performance. The behavior and uptake of the column might be examined by examining the effect of different operating circumstances on the breakthrough curve and column performance. The fitting technique included determining the constants for each breakthrough model, including Yoon-Nelson and Thomas. The phosphate and nitrate τ values range from 46.23 to 118.63 min and 38.62 to 100.52 min, respectively, and the phosphate and nitrate q_o values range from 8.63 to 33.54 mg/g and 7.45 to 26.80 mg/g, respectively. The models' speed constants were shown to grow with increasing flow rates, indicating that the adsorption kinetics are controlled by mass transfer from outside the system. The results obtained from the fixed-

bed column experiments indicate that the material can be effectively applied in continuous wastewater treatment systems. The relatively high adsorption capacity and delayed breakthrough time suggest good column performance and longer operational lifetime.

Funding: This study was conducted without any specific grant from public, commercial, or not-for-profit funding agencies.

Authors' contributions Sally A. Hussein: Data curation, investigation, writing—original draft, writing-review, and editing. Muthanna J. Ahmed: Supervision and Editing.

Declaration of Competing Interest The authors declare that they have no known competing financial interests or personal relationships that could have appeared to influence the work reported in this paper.

Data availability: All relevant data are included in the paper.

References

[1] Z. A. Ibrahim and A. F. Al-Alawy, "Synthesis of Magnetic Nanoparticles Coated with Chitosan and Silicon Dioxide as Smart Draw Solutions in Forward Osmosis Process," *Chemistry Africa journal*, vol. 8, no. 7, pp. 2943–2957, Sep. 2025, https://doi.org/10.1007/s42250-025-01313-0

[2] Z. A. Ibrahim and A. F. Al-Alawy, "Synthesis and characterization of dual functional potassium doped MWCNT composites (K@Fe3O4@MWCNT and TEG-K/MWCNT) as innovative osmotic agents for forward osmosis processes," *Journal of Molecular Liquids*, vol. 437, Nov. 2025, https://doi.org/10.1016/j.molliq.2025.128452

[3] Y. Endale, A. B. Bayu, Z. A. Samuel, S. Kebede, and E. Kulbat, "Optimizing Citrullus lanatus seed-based coagulation for enhanced phosphate and nitrate removal from agricultural wastewater," *Scientific African*, vol. 28, Jun. 2025, https://doi.org/10.1016/j.sciaf.2025.e02686

[4] K. Velusamy *et al.*, "Advanced techniques to remove phosphates and nitrates from waters: a review," Aug. 01, 2021, *Springer Science and Business Media Deutschland GmbH*. https://doi.org/10.1007/s10311-021-01239-2

[5] E. Priya, S. Kumar, C. Verma, S. Sarkar, and P. K. Maji, "A comprehensive review on technological advances of adsorption for removing nitrate and phosphate from waste water," *Journal of Water Process Engineering*, vol. 49, Oct. 01, 2022, https://doi.org/10.1016/j.jwpe.2022.103159

[6] A. Gizaw, F. Zewge, A. Kumar, A. Mekonnen, and M. Tesfaye, "A comprehensive review on nitrate and phosphate removal and recovery from aqueous solutions by adsorption," *Water Infrastructure, Ecosystems and Society*, vol. 70, no. 7, Nov. 01, 2021, *IWA Publishing*. https://doi.org/10.2166/aqua.2021.146

[7] K. R. Burow, B. T. Nolan, M. G. Rupert, and N. M. Dubrovsky, "Nitrate in groundwater of the United States, 1991-2003," *Environmental Science and Technology*, vol. 44, no. 13, pp. 4988–4997, Jul. 2010, https://doi.org/10.1021/es100546y

[8] R. a, S. Chhikara, and P. Kumar, "Biosorption for Removal of Nitrates and Phosphates: A Review," *International Advanced Research Journal in Science, Engineering and Technology*, vol. 8, no. 8, Aug. 2021, https://doi.org/10.17148/iarjset.2021.88102

[9] P. Karthikeyan, S. S. D. Elanchezhiyan, J. Preethi, S. Meenakshi, and C. M. Park, "Mechanistic performance of polyaniline-substituted hexagonal boron nitride composite as a highly efficient adsorbent for the removal of phosphate, nitrate, and hexavalent chromium ions from an aqueous environment," *Applied Surface Science*, vol. 511, May 2020, https://doi.org/10.1016/j.apsusc.2020.145543

[10] H. A. T. Banu, P. Karthikeyan, and S. Meenakshi, "Removal of nitrate and phosphate ions from aqueous solution using zirconium encapsulated chitosan quaternized beads: Preparation, characterization and mechanistic performance," *Results in Surfaces and Interfaces*, vol. 3, May 2021, https://doi.org/10.1016/j.rsurfi.2021.100010

[11] J. Castañeda-DÍaz, T. Pavón-Silva, E. Gutiérrez-Segura, and A. Colín-Cruz, "Electrocoagulation-Adsorption to Remove Anionic and Cationic Dyes from Aqueous Solution by PV-Energy," *Journal of Chemistry*, vol. 2017, 2017, https://doi.org/10.1155/2017/5184590

[12] Y. Ye, Y. Ren, J. Zhu, J. Wang, and B. Li, "Removal of nitrate and Cr(VI) from drinking water by a macroporous anion exchange resin," *Desalination and Water Treatment*, vol. 57, no. 55, pp. 26427–26439, Nov. 2016, https://doi.org/10.1080/19443994.2016.1164081

[13] S. A. Hussein and M. J. Ahmed, "Batch and fixed-bed adsorption of phosphate and nitrate on char derived by the co-pyrolysis of waste tires and corn cobs," *International Journal of Renewable Energy Development*, vol. 15, no. 1, pp.1-15, 2026, https://doi.org/10.61435/ijred.2026.61629

[14] A. S. Abbas and S. A. Hussien, "Equilibrium, Kinetic and Thermodynamic Study of Aniline Adsorption over Prepared ZSM-5 Zeolite," *Iraqi Journal of Chemical and Petroleum Engineering*, vol. 18, no. 1, pp. 47–56, 2017, https://doi.org/10.31699/IJCPE.2017.1.4

[15] Z. N. Jamka, W. T. Mohammed, Z. YOU, and H. R. Abid, "Enhancing Nitrate Ion Removal from Water using Fixed Bed Columns with Composite Chitosan-based Beads," *Iraqi Journal of Chemical and Petroleum Engineering*, vol. 24, no. 4, pp. 75–81, Dec. 2023, https://doi.org/10.31699/ijcpe.2023.4.7

[16] R. Gouran-Orimi, B. Mirzayi, A. Nematollahzadeh, and A. Tardast, "Competitive adsorption of nitrate in fixed-bed column packed with bio-inspired polydopamine coated zeolite," *Journal of Environmental Chemical Engineering*, vol. 6, no. 2, pp. 2232–2240, Apr. 2018, https://doi.org/10.1016/j.jece.2018.01.049

[17] A. Adauto and M. R. Sun-Kou, "Comparative study of anion removal using adsorbents prepared from a homoionic clay," *Environmental Nanotechnology Monitoring and Managment*, vol. 15, May 2021, https://doi.org/10.1016/j.enmm.2021.100476

[18] Z. N. Jamka and W. T. Mohammed, "Parametric and kinetic study of nitrate removal from water by modified chitosan composite beads," *Chemistry and Chemical Technology*, vol. 18, no. 1, pp. 83–93, 2024, https://doi.org/10.23939/chcht18.01.083

[19] K. Vijayaraghavan and R. Balasubramanian, "Application of pinewood waste-derived biochar for the removal of nitrate and phosphate from single and binary solutions," *Chemosphere*, vol. 278, Sep. 2021, https://doi.org/10.1016/j.chemosphere.2021.130361

[20] S. P. Singh Yadav *et al.*, "Biochar application: A sustainable approach to improve soil health," *Journal of Agriculture and Food Research*, vol 11, Mar. 01, 2023, https://doi.org/10.1016/j.jafr.2023.100498

[21] V. Steffen, M. S. de Oliveira, L. da Silva Pego Hericks, S. W. Alberti, M. H. da Silva, and E. A. da Silva, "Corn cob pyrolysis: A systematic literature review of methods and applications," *The Canadian Journal of Chemical Engineering*, vol. 103, no. 11, 2025, https://doi.org/10.1002/cjce.25707

[22] H. Ghai *et al.*, "An Overview on Co-Pyrolysis of Biodegradable and Non-Biodegradable Wastes," *Energies*, vol. 15, Jun. 01, 2022, *MDPI*. https://doi.org/10.3390/en15114168

[23] Y. H. E. E. YOON and J. H. and NELSON, "Application of Gas Adsorption Kinetics I. A Theoretical Model for Respirator Cartridge Service Life," *American Industrial Hygiene Association Journal*, vol. 45, no. 8, pp. 509–516, Aug. 1984, https://doi.org/10.1080/15298668491400197

[24] H. C. Thomas and B. C. Henry Thomas Vol, "Heterogeneous Ion Exchange in a Flowing System." *Journal of the American Chemical Society*, vol. 66, 1944, https://doi.org/10.1021/ja01238a017

[25] N. Cheng, B. Wang, Q. Feng, X. Zhang, and M. Chen, "Co-adsorption performance and mechanism of nitrogen and phosphorus onto eupatorium adenophorum biochar in water," *Bioresource Technology*, vol. 340, Nov. 2021, https://doi.org/10.1016/j.biortech.2021.125696

[26] J. Yang, H. Li, D. Zhang, M. Wu, and B. Pan, "Limited role of biochars in nitrogen fixation through nitrate adsorption," *Science of the Total Environment*, vol. 592, pp. 758–765, Aug. 2017, https://doi.org/10.1016/j.scitotenv.2016.10.182

[27] Z. Huang *et al.*, "Co-adsorption performance and mechanism of ammonium and phosphate by iron-modified biochar in water," *Journal of Water Process Engineering*, vol. 67, Nov. 2024, https://doi.org/10.1016/j.jwpe.2024.106209

[28] M. Konneh, S. M. Wandera, S. I. Murunga, and J. M. Raude, "Adsorption and desorption of nutrients from abattoir wastewater: modelling and comparison of rice, coconut and coffee husk biochar," *Heliyon*, vol. 7, no. 11, Nov. 2021, https://doi.org/10.1016/j.heliyon.2021.e08458

[29] W. T. Mohammed and S. A. Rashid, "Phosphorus removal from wastewater using oven-dried alum sludge," *International Journal of Chemical Engineering*, 2012, https://doi.org/10.1155/2012/125296

[30] H. Abdipour, G. Asgari, A. Seid-Mohammadi, A. Rahmani, and R. Shokoohi, "Investigating the efficiency of fixed bed column containing Fe3O4-ZIF8@eggshell membrane matrix in concurrent adsorption of arsenic and nitrate from water," *Ecotoxicology and Environmental Safety*, vol. 288, Dec. 2024, https://doi.org/10.1016/j.ecoenv.2024.117359

[31] N. Baboli and A. Bafkar, "Nitrate removal from aqueous solutions using nanostructured adsorbents in continuous and discontinuous systems," *Desalination and Water Treatment*, vol. 284, pp. 116–133, Feb. 2023, https://doi.org/10.5004/dwt.2023.29164

[32] J. Wang, Y. Amano, and M. Machida, "Nitrate removal from aqueous solution by glucose-based carbonaceous adsorbent: Batch and fixed-bed column adsorption studies," *Colloids and Surfaces: A Physicochemical and Engineering Aspects*, vol. 686, Apr. 2024, https://doi.org/10.1016/j.colsurfa.2024.133296

[33] A. Olgun, N. Atar, and S. Wang, "Batch and column studies of phosphate and nitrate adsorption on waste solids containing boron impurity," *Chemical Engineering Journal*, vol. 222, pp. 108–119, Apr. 2013, https://doi.org/10.1016/j.cej.2013.02.029

[34] T. M. Darweesh and M. J. Ahmed, "Adsorption of ciprofloxacin and norfloxacin from aqueous solution onto granular activated carbon in fixed bed column," *Ecotoxicology and Environmental Safety*, vol. 138, pp. 139–145, Apr. 2017, https://doi.org/10.1016/j.ecoenv.2016.12.032

[35] J. A. Palangi, M. A. Gholami Sefidkouhi, and M. A. Bahmanyar, "Effect of surfactant concentration on zeolite modification for nitrate removal and its simulation with kinetics models and ANFIS in fixed-bed column," *Journal of Water and Wastewater*, 30, no. 3, pp 73-86. 2019, https://doi.org/10.22093/wwj.2018.110863.2567

[36] T. Pratap, A. K. Chaubey, S. Kapoor, B. Preetiva, and D. Mohan, "Fixed-Bed Adsorption System Design Models for Groundwater Nitrate Removal Using Acid-Modified Biochar Developed from Invasive Prosopis juliflora Bark," *ACS Sustainable Resource Management*, vol. 2, no. 4, pp. 572–580, 2025, https://doi.org/10.1021/acssusresmgt.4c00371

أمتصاص العناصر الغذائية من النترات والفوسفات في طبقة ثابتة باستخدام الفحم المحضر عن طريق التحلل الحراري المشترك لإطارات النفايات ونواة التمر

سالي علي حسين [١،*]، مثنى جبار احمد [١]

١ قسم الهندسة الكيمياوية، كلية الهندسة، جامعة بغداد، بغداد، العراق

الخلاصة

يُعدّ تحويل إطارات السيارات المستعملة ونوى التمر إلى فحم نباتي عبر التحلل الحراري المشترك طريقة فعّالة لإزالة هذه المواد وإعادة تدويرها بأمان. اختبرت هذه الدراسة الفحم النباتي كمادة ماصة منخفضة التكلفة لإزالة النترات والفوسفات في أنظمة ذات طبقة ثابتة، مما يوفر طريقة لإعادة استخدام إطارات السيارات المستعملة ونوى التمر. تم قياس تأثير تركيز الملوثات الداخلة (٥٠، ١٥٠، و٣٠٠ ملغم/لتر)، ومعدل التدفق (٥، ١٠، و١٥ مل/دقيقة)، وارتفاع الطبقة (٥، ١٠، و١٥ سم) على اختراق نظام الامتزاز. تم تحليل خصائص الفحم النباتي باستخدام مطيافية الأشعة تحت الحمراء بتحويل فوريه (FTIR)، وقياس مساحة السطح النوعية (BET)، وقياس جهد زيتا. أظهر تحليل الطبقة الثابتة توافقًا ممتازًا لبيانات الاختراق مع كلٍ من نموذجي يون–نيلسون وتوماس. في ظل ظروف مختلفة، اتفقت النتائج مع نموذجي يون–نيلسون وتوماس، وذلك وفقًا لقيم معامل الارتباط R^2 (٠,٨١٤٧–٠,٩٩١٣) للفوسفات، و(٠,٩١٨٧–٠,٩٩١٣) للنترات، و(٠,٨١٤٦–٠,٩٩٠٧) للفوسفات، و(٠,٩١٨٩–٠,٩٨٠١) للنترات، على التوالي. تُظهر هذه النتائج إمكانية استخدام الفحم المُحضر كمادة ماصة فعالة ومستدامة لإزالة المغذيات في أنظمة المعالجة المستمرة، مما يوفر نهجًا واعدًا لمعالجة مياه الصرف الصحي واستغلال النفايات.

الكلمات الدالة: امتزاز الطبقة الثابتة، منحنيات الاختراق، الملوثات الثنائية، امتزاز الأنيونات، الانحلال الحراري المشترك.